Exp Brain Res (2000) 132:419–433
Digital Object Identifier (DOI) 10.1007/s002210000366

RESEARCH ARTICLE

K.E. Novak · L.E. Miller · J.C. Houk

Kinematic properties of rapid hand movements in a knob turning task

Received: 26 October 1999 / Accepted: 28 January 2000 / Published online: 25 March 2000

Abstract In order to understand how the central nervous system controls the kinematics of rapid finger and hand movements, we studied the motions of subjects turning a knob to light-emitting diode targets, similar to tuning a radio dial. On many trials, subjects turned the knob with a single, smooth, and regular motion as revealed by the angular position and velocity trajectories, but on others, subjects produced irregularities in the kinematics. Like many past studies, we interpreted these irregularities as discrete corrective submovements. Unlike other studies, we used a direct, objective algorithm to identify overlapping submovements, detecting appreciable inflections in the acceleration traces by examining zero crossings in their derivatives, jerk and snap. The movements without overlapping submovements on average had a near symmetric, bell-shaped velocity profile that was independent of speed, and which matched the theoretical minimum jerk velocity very closely. We proposed three plausible mechanisms for altering the shape of movement kinematics, and implemented a mass-spring model with nonlinear damping to explore the possibilities. Although there was relatively little variability in the shape and symmetry of movements across trials, there was a fair amount of variability in their amplitude. We show that subjects attempted to eliminate the need for corrective submovements by making more accurate primary movements with practice, but that the variability inherent in rapid movements dictated the need for corrective submovements. Subjects used corrective submovements to improve final endpoint accuracy while reducing endpoint variability, resulting in higher task success rates.

Key words Hand movements · Kinematics · Symmetry · Submovements · Model

K.E. Novak (✉) · L.E. Miller · J.C. Houk
Department of Physiology, Northwestern University,
2145 Sheridan Road, Evanston, IL 60208-3107, USA
e-mail: k-novak@nwu.edu

K.E. Novak · J.C. Houk
Department of Biomedical Engineering, Northwestern University,
303 E. Chicago Avenue, Ward 5–150, Chicago, IL 60611, USA

Introduction

Every day we use our hands and fingers to grasp and manipulate objects in our environment with incredible coordination and skill. A disproportionate amount of the brain's motor cortex is devoted to these complicated hand skills necessary for interacting with the world around us. To gain insight into how we use our hands to manipulate objects and how we achieve accuracy in rapid hand movements, this study investigates the kinematics of a coordinated multijoint hand manipulation task. Subjects were required to turn a knob rapidly to align a pointer with a target. The movement was complicated, with the possibility of eighteen degrees of freedom with all the finger joints.

In studying the kinematic features of simpler movements, some investigators (Abend et al. 1982; Atkeson and Hollerbach 1985; Flash and Hogan 1985; Gordon et al. 1994; Morasso 1981; Uno et al. 1989) have observed smooth, nearly symmetric movement trajectories. Others (Berthier 1996; Crossman and Goodeve 1983; Flash and Henis 1990; Keele 1968; Krebs et al. 1998; Lee et al. 1997; Meyer et al. 1988; Milner 1992; Morasso and Mussa Ivaldi 1982; Pratt et al. 1994; Woodworth 1899) have described irregularities in movements produced as a series of discrete submovements, or substantial asymmetries in the trajectories (Moore and Marteniuk 1986; Nagasaki 1989; Wiegner and Wierzbicka 1992). Many movements contain irregularities and multiple velocity peaks near the end of a movement when high spatial precision is required (Crossman and Goodeve 1983).

The iterative-corrections model of Keele (1968) and Crossman and Goodeve (1983) proposed that a series of submovements of a constant movement time and successively smaller amplitudes were generated one after the other until the target was reached. Meyer et al. (1988) recognized a shortcoming of this model in its inability to deal with movement variability, and proposed a "stochastic optimized-submovement model." In this model one or more submovements may be made after the pri-

mary movement, depending on the accuracy of the noisy initial submovement. Other investigators have used a similar approach of multiple submovements, but allowed the submovements to overlap on top of each other. Several kinds of movements have been analyzed as a set of overlapping submovements of the same scaled shape, including handwriting (Morasso and Mussa Ivaldi 1982), "double step" planar arm reaching movements (Flash and Henis 1990), freeform reaching to place pegs into a peg-board (Milner 1992), infant reaching to a target (Berthier 1996), and manual interception of a moving target (Lee et al. 1997).

While these prior studies offer explanations for a wide range of motor behaviors as sequences of discretely commanded submovements, there is as yet no established method for objectively identifying the occurrences of overlapping submovements. Previous approaches have relied on an assumption of minimum-jerk trajectories (Berthier 1996; Flash and Henis 1990), subjectively defined initial guesses for submovement parameters (Lee et al. 1997) or subjective fits to changes in the direction of hand path (Milner 1992). In the present study, we offer new objective criteria for identifying the occurrences of overlapping submovements, and we use this methodology to select movements that are not contaminated by overlapping submovements. The kinematics of the latter are then thoroughly analyzed.

Preliminary descriptions of this work have appeared elsewhere (Novak et al. 1996a,b).

Materials and methods

Subjects

Six subjects participated in this study with their informed consent, according to the university protocol for human research subjects. They had no history or symptoms of neurological disease and appeared to be healthy individuals with normal motor skills. They ranged in age from 24 to 50 years. Five were male and one was female. One was left handed, while the others were right handed.

Apparatus, task, and protocol

Subjects were seated in a chair facing the apparatus with their dominant arm on the chair's arm rest. Subjects grasped a deeply grooved knob (Fig. 1A) attached to a motor shaft mounted on a metal rack. Protruding from the knob was a pointer with a light-emitting diode (LED) on its tip. Surrounding the tip of the pointer in a semicircle above the knob were LED targets spaced 10° apart, as shown in the schematic of the apparatus in Fig. 1A. For a given experiment, a set of three of these LED targets was used (shaded and labeled 1, 2, and 3 in Fig. 1A), each spaced 30° apart. The subjects' task was to turn the knob quickly and accurately with their dominant hand to align the pointer with the lighted target.

Figure 1B shows a single trial in which a subject moved the pointer from target 3 (shaded region at –30°) to target 2 (shaded area at 0°). After a fixed hold time (0.5 s) at the current lighted LED target (target 3), a new target (target 2) was chosen pseudorandomly and then illuminated, cueing subjects to move. To complete the trial successfully and receive a brief tone functioning as a reward, subjects were required to move the pointer to acquire the target within 0.4 s, and to remain in the target zone for an additional 0.5 s. In addition to these time constraints, there was an accuracy constraint of 8°, the width of the target window. While the target width was constant, the distance to the target was either 30° or 60°.

Experiments were performed in a darkened room so that subjects could see only the illuminated LEDs on the knob pointer and target. The pointer LED was extinguished as soon as subjects began to move and was returned after the trial was completed. Re-

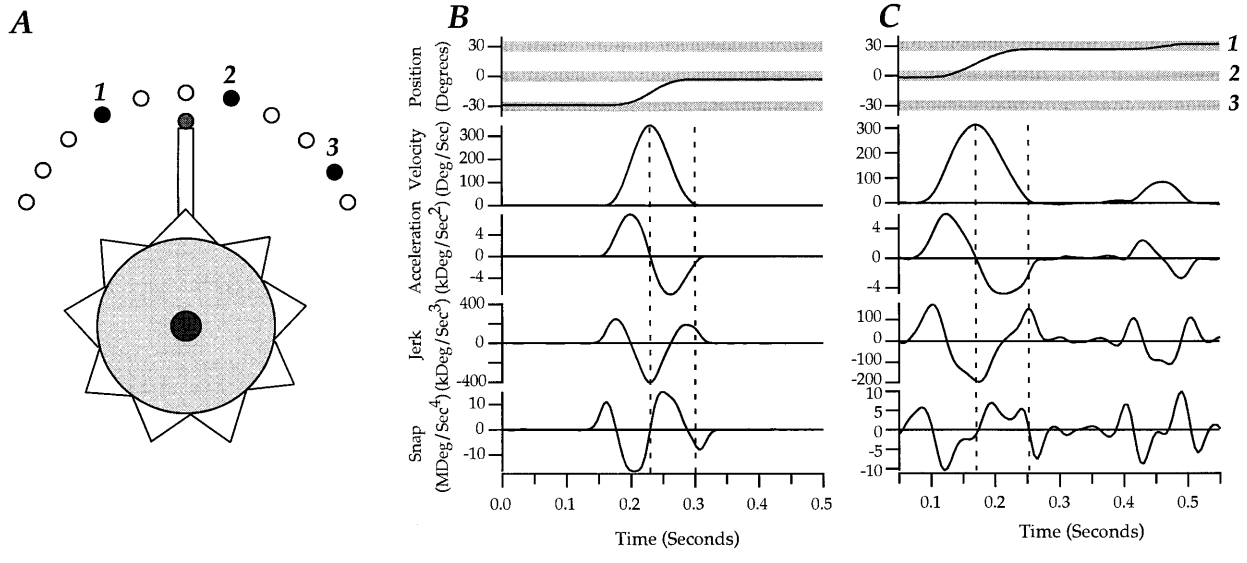

Fig. 1 **A** Schematic of knob turning apparatus. Subjects align the knob pointer with a light-emitting diode (LED) to one of three LED targets (*dark circles labeled 1, 2, 3*) above the pointer by rapidly twisting the knob with their hand and fingers. **B** Kinematic traces from one trial, showing the movement over time along with its successively higher time derivatives below: velocity, acceleration, jerk, and snap. The position trace is shown on *top*, as the subject moves from target 3 at –30° (*shaded region*) to target 2 at 0°. The *vertical dashed lines* represent the time of peak velocity of the primary movement, and the end of the initial movement, when velocity settled near zero. Trials **B** and **C** were made as a single primary movement, with smooth and regular kinematics. There was only one deceleration pulse accompanied by one jerk zero crossing and one snap zero crossing during the second half of the movement. **C** A single primary movement, followed by a delayed submovement 150 ms later

moving visual feedback ensured that any feedback-based corrections that may have been generated were based on proprioceptive and not visual cues.

The subjects performed trials in blocks of 240, lasting approximately 8–10 min. In between sets the lights were turned on, preventing subjects' eyes from adapting to the darkness. Subjects confirmed that they were unable to see anything besides the LEDs of the knob pointer and the targets throughout each set of trials in the dark. Subjects rested as long as they wanted between sets, typically 3 or 4 min. The whole experiment consisted of four or five blocks of trials lasting between 45 min and 1 h.

As subjects performed the task, the angular position of the knob pointer was measured from a potentiometer attached to the shaft of the motor. Likewise, the angular velocity was transduced by a tachometer coupled to the same axis of rotation. The position and velocity signals were sampled by the computer at 200 samples/s for storage and later analysis. Higher-order derivatives, including acceleration, jerk, and snap, were obtained for each trial by numerical differentiation. Digital filtering and analysis was performed using the Igor Pro software package (Wavemetrics). Velocity and its derivatives were filtered with a three sample sliding box-car filter.

Data analysis

The timing of movement onset, peak velocity, and the end of the movement were detected for each trial. Movement onset was defined as the time when velocity increased past a threshold value of 10% of the peak velocity (around 30–50°/s). The time of peak velocity of the initial movement was usually found by detecting when the acceleration first crossed zero from positive to negative. However, in about 5% of all trials, the acceleration trace had an inflection before the zero crossing, indicating the occurrence of a second acceleration pulse. When the first acceleration pulse was interrupted in this way, the time of peak velocity of the initial movement was estimated as the time of the acceleration inflection (determined by the jerk zero crossing), instead of the acceleration zero crossing. This estimate of the primary movement peak velocity time was usually 5–10 ms before the true time of the peak velocity of the initial movement, when the first acceleration pulse would have crossed zero if not obscured by the second acceleration pulse.

The end of the movement was detected in two ways, as required for two different applications. Firstly and similar to movement onset, the end of the movement was defined as the time when velocity crossed below a threshold value equal to 10% of the peak velocity. This method prevented symmetry in the movement from being distorted. The next estimate of the end of the movement was used to guarantee that the movement really stopped after it slowed down. The second definition was the time when velocity crossed below a threshold of ±10°/s and stayed there for at least 30 ms. This second method was used in the analysis of the regularity of movements, described below.

Movement irregularities were detected as appreciable inflections in the acceleration during the second half of the movement. Inflections in the acceleration were found by counting the zero crossings of the derivative of acceleration, jerk, and its derivative, snap. Irregular trials had more than a single jerk or snap zero crossing during a time window during the second half of the movement. The time window began 12 ms after the peak velocity in order to exclude the snap zero crossing at peak velocity. The window ended 2 ms after the velocity crossed under the 10°/s threshold and settled to zero. The 2 ms were added to include the snap zero crossings associated with sharp final decelerations. The vertical dashed lines in Figs. 1 and 2 represent the peak velocity and the time the movement velocity settled to zero, without the window adjustments noted above.

In order to quantify the symmetry and shape of the angular velocity profiles, the parameters K and C were used, following Nagasaki (1989) and Soechting (1984), respectively. K represents the "relative time to peak velocity or relative duration of acceleration." Time-symmetric movements have a K=0.5. Movements with short accelerations relative to deceleration have a K<0.5, while those with relatively long accelerations have a K>0.5. The parameter C is equal to the ratio of the peak velocity to the average velocity of a movement. The C value of a movement velocity profile is a measure of the shape irrespective of movement amplitude or duration.

Several measures of performance were used, one being the trial success rate. Another performance metric was the mean squared jerk. A final useful performance metric was the endpoint error, computed as the signed distance of the pointer from the center of the target at the end of the movement, defined as the time when velocity decreased below 10% of the peak velocity. Positive errors indicate movements past the target, while negative errors represent movements ending short of the target. Using the velocity threshold of 10% of the peak velocity excluded small drifts before or after the main portion of the movement, but introduced a small bias in the estimate of the duration and amplitude of the movement. Compared with a fixed threshold of 10°/s, the 10% of peak velocity criterion estimated the amplitude of the movement 2% smaller than it actually was, and the duration 15% shorter.

The performance metrics for each subject were computed for each block of 240 trials. To test whether or not each subject's performance significantly improved from the first run to the last during practice, three statistical tests were used. Student's one-tailed *t*-test was used to compare the equality of means of reaction time, movement time, peak velocity, mean squared jerk, and endpoint error from the beginning to the end. For metrics describing a percentage of trials, a test for equality of proportions was used with a minor modification of the *t*-test. The test estimates the variance as the average percentage for both runs times one minus the average percentage. To test the standard deviation of the endpoint errors for significant changes, the *F* statistic was used. All tests were performed at the 0.05 significance level.

Non-linear mass-spring model of movement

In order to better understand how changes in the kinematics of rapid movements may be explained by changes in the central motor command, a mass-spring model of movements with non-linear damping was explored. The model was modified slightly from its original form describing the intrinsic and reflex properties of motion of the human wrist (Gielen et al. 1984; Wu et al. 1990). The wrist joint was modeled as a mass (M) and spring (k) with a variable slack length (x_{eq}) and non-linear viscous damping (b):

$$M\ddot{x} + b\dot{x}^{1/5} + k(x - x_{eq}) = 0 \quad (1)$$

Parameters of M=1, b=3, and k=30 were chosen in a previous study (Barto et al. 1999) to give movements which qualitatively resemble those recorded in the wrist (Wu et al. 1990). This model has been used by Houk, Barto, and colleagues as a simplified motor plant that a biologically inspired cerebellar neural network controller learned to control (Barto et al. 1999; Buckingham et al. 1994, 1995).

The model produces position and velocity outputs based on varying amplitude and duration pulse-step command inputs (i.e., setting the slack length of the spring, x_{eq}). The square pulse-step command was low-pass filtered with a time constant of 20 ms, resembling the time constant of the neuromusculoskeletal activation dynamics. The Matlab/Simulink computing environment (Mathworks) was used to implement the model.

Results

Subjects made rapid hand movements to align the knob pointer to an 8°-wide target 30° or 60° away. They sometimes achieved the required accuracy with a single primary movement (Fig. 1B), but often they needed to gen-

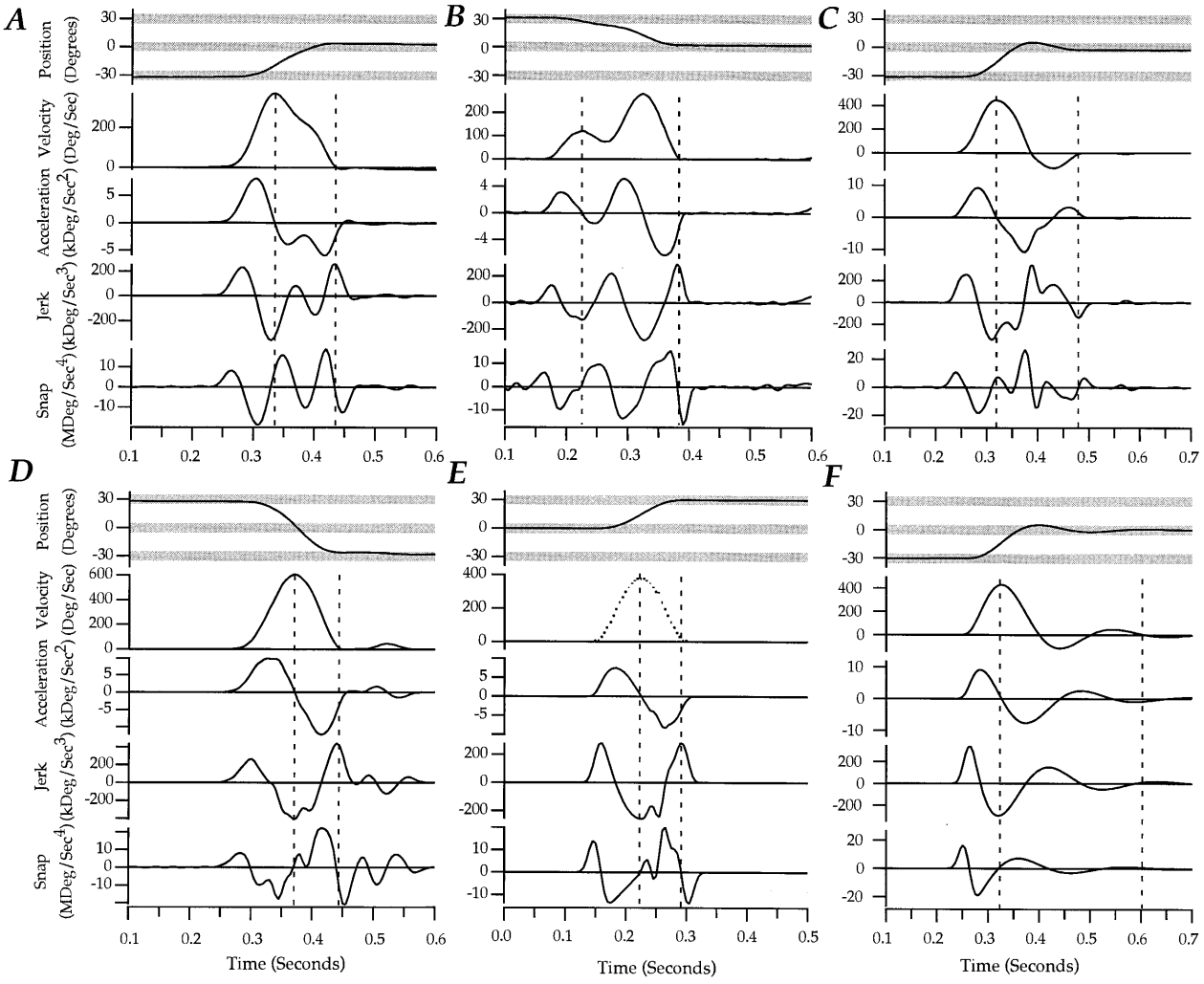

Fig. 2A–F Sample trials showing irregularities caused by submovements overlapping the primary movement, and the method for detecting these irregularities based on jerk and snap zero crossings. Plots are the same as Fig. 1B,C. **A–C** Trials with inflections in the acceleration trace during the second half of the primary movement (between *dashed vertical lines*), indicated by more than one zero crossing and more than one snap zero crossing. These irregularities are caused by submovements overlapping the primary movement. **D** An example of an insignificant inflection in the acceleration which caused a spurious zero crossing in the snap trace. Since the snap peak created by the zero crossing was not very large, this trial was considered a single primary movement, with a little bit of noise contributing to small irregularities in the higher derivatives. **E** The effect of noise on the velocity trace on the numerical differentiation process is shown. One sample point at 0.245 s was artificially increased by 5 A/D bits to produce the snap zero crossing and snap peak required to count a snap zero crossing as significant and not due to noise. **F** A simulation of the step response of a linear, third-order system with the transfer function: $G(s)=\omega_n^2/(s^2+2\zeta\omega_n s+\omega_n^2)*\tau/(s+\tau)$. The damping coefficient, ζ, was 0.3, the movement amplitude was 30°, and the duration 95 ms. The natural frequency, ω_n, was derived as $\omega_n=\pi/(\text{time to peak amplitude}*(1-\zeta^2)^{1/2})$. The equation of the step response was: $\text{position}(t)=\text{amplitude}*(1-(e^{-\zeta\omega nt})/(1-\zeta^2)^{1/2})*\sin(\omega_n(1-\zeta^2)^{1/2}t+\text{atan}((1-\zeta^2)^{1/2}/\zeta)$. The step input was first filtered with a first-order low-pass filter with a cutoff frequency of 4 Hz, equivalent to a 40-ms time constant (τ) that may be associated with activation dynamics. This extra filter was needed to match the initial response of the higher-order derivatives. The derivatives of position were calculated numerically. Note how an underdamped linear second-order system oscillates with a fixed frequency, $\omega_d=\omega_n*(1-\zeta^2)^{1/2}=1/(2*\text{time to peak velocity})=3.33$ Hz, whereas the actual trial in **C** does not oscillate

erate corrective submovements. When submovements were delayed until after the primary movement ended (Fig. 1C), they were easy to identify. In attempting to achieve the speed requirement, however, subjects often generated submovements before the primary movement ended. We used zero crossings of higher time derivatives of the movement as objective criteria for detecting trials that had irregularities produced by overlapping submovements (Fig. 2A–C). These criteria allowed us to divide the individual trials into three categories: (1) pure primary movements, (2) primary movements followed by delayed submovements, and (3) primary movements with overlapping submovements. Figure 3 shows the incidences of these three categories in 30° and 60° trials for each of the six subjects.

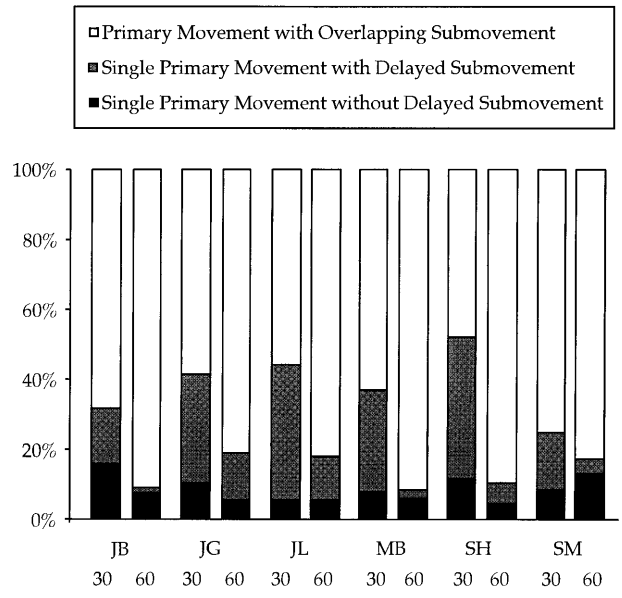

Fig. 3 Classification of trials based on the number and time of occurrence of submovements, for each subject and amplitude of movement (30° or 60°). The percentage of each trial type is shown: trials with a primary movement and an overlapping submovement are *white*, trials with a single primary movement and a delayed submovement are *gray*, and trials with only a single primary movement are in *black*

Detection of overlapping submovements

Unlike the smooth and regular movements in Fig. 1, subjects often made movements with irregular kinematics, like the trials illustrated in Fig. 2A–C. We interpret the irregularities in these movements, like the dual velocity peak in Fig. 2B, as being caused by submovements that are superimposed on an initial primary movement. Because each submovement is generated by a discrete torque pulse, each submovement of significant amplitude will cause an inflection in the angular acceleration of the movement. By looking at the first two derivatives of acceleration, jerk and snap, irregularities caused by discrete submovements can be detected. Jerk and snap are plotted below the acceleration traces in Figs. 1 and 2.

The smooth and regular movement of Fig. 1B was generated with one acceleration pulse and one deceleration pulse, and contained only one jerk zero crossing and one snap zero crossing during a time window from the peak velocity (first dashed vertical line) to the end of the movement (second dashed vertical line). The time window was shortened to begin 12 ms after the peak velocity in order to exclude the snap zero crossing right at the peak velocity. In contrast to the single, smooth deceleration pulse of Fig. 1B, the movement in Fig. 2A showed an inflection in the deceleration, with two peaks caused by the two peaks in the velocity profile. Instead of the single jerk zero crossing during the second half of the movement, there were three jerk zero crossings and three snap zero crossings, documenting the irregularity of the movement.

Similar to the trial of Fig. 2A, during the movement in Fig. 2B the subject clearly made two submovements which overlapped in time. The acceleration trace had a deceleration peak that was smaller than usual, followed by another acceleration and another deceleration peak from the overlapping submovement. This trial was irregular and had three jerk and snap zero crossings during the second portion of the movement.

A subject produced a different kind of movement irregularity on the trial of Fig. 2C. Instead of smoothly decelerating to zero velocity, the movement went past the final endpoint, reversed directions, and then stopped. The acceleration trace from peak velocity to the end of the movement (between the dashed lines) was not a single, regular pulse, but instead contained two significant inflections and an extra positive acceleration pulse.

The trial of Fig. 2C cannot be simply explained as an underdamped movement. Figure 2F shows a simulated trial using an underdamped, third-order model. Although this simulated trial has about the same amount of overshoot as the actual trial in Fig. 2C, the simulated trial continues to oscillate after the first overshoot. Another major difference is that the simulated trial has smooth acceleration pulses with no inflections or irregularities in the jerk or snap traces.

To counteract the effect of noise amplified through numerical differentiation, only significant snap zero crossings that created large snap peaks were counted, with a magnitude of at least $2\times10^{6}°/s^{4}$. If the snap just barely crossed zero with a small peak value before crossing again, as in the trial of Fig. 2D, it was not included as a snap zero crossing. On this trial, just 25 ms after the peak velocity, the tiny inflection in the acceleration trace and the noisy differentiation caused the snap to briefly cross zero. This trial had only one significant snap zero crossing, and was categorized as smooth and regular. A single sample point with a spike of noise on the velocity signal, equivalent to 5 bits of the possible 11 bits of A/D converter resolution was required to produce this level of snap accidentally. Figure 2E demonstrates the effect on snap made by adding 5 bits, or 26°/s, of noise to a single sample point at time 0.255 s. It takes a fairly large amount of noise to produce false movement irregularities.

Using the method of jerk and snap zero crossings to detect movement irregularities provided an objective and automatic means for determining when a primary movement was contaminated by an overlapping submovement. The trials without overlapping submovements were further separated based on whether or not they contained a delayed submovement. The percentages of the three categories of trial shown in Fig. 3 were based on these criteria. Note that for the large movements in particular, several subjects used the strategy of a large primary movement and a smaller homing-in overlapping submovement near its end. While there were some differences between subjects, on average subjects produced submovements which temporally overlapped the primary movement on nearly two-thirds of the trials. For the re-

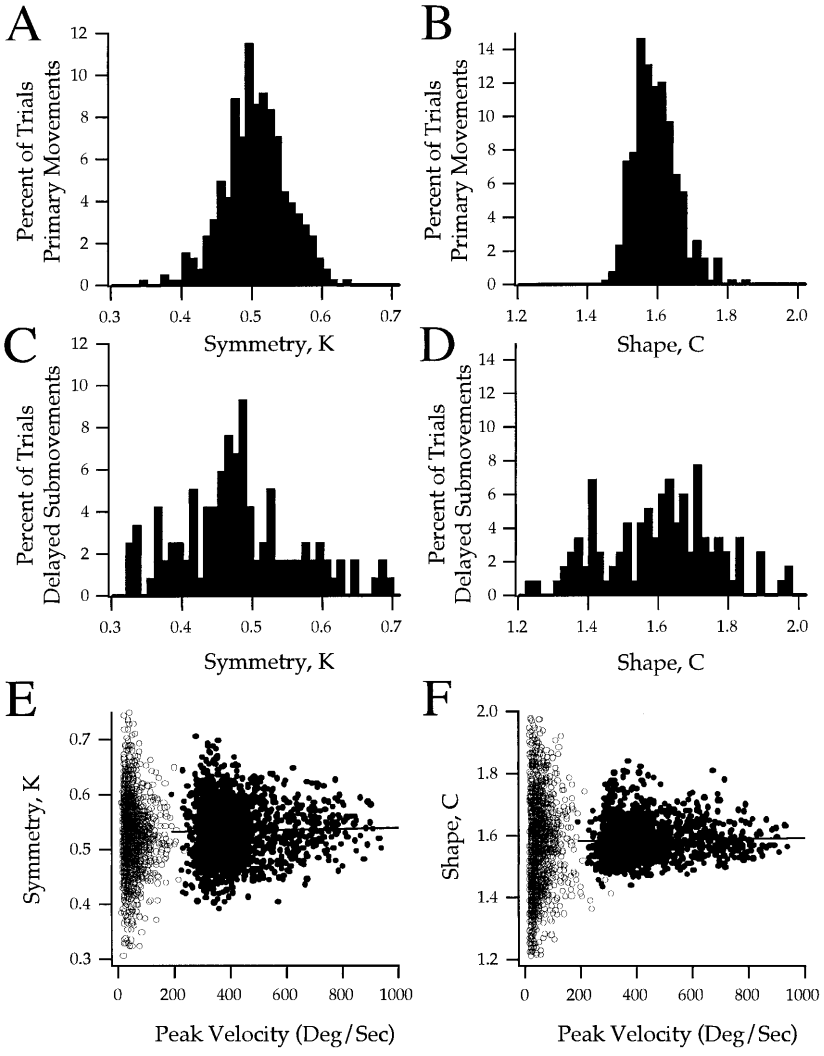

Fig. 4A–F K and C values. **A–D** Histogram of the K (time symmetry) and C (ratio of peak velocity to mean velocity) values of the single primary movement velocity profiles (**A,B**) and pure delayed submovement (**C,D**) velocity profiles for subject SH. **E,F** Scatter plot of K and C versus peak velocity for all trials from all subjects, showing a lack of correlation between the shape of the velocity profile and the speed of movement. Filled circles represend primary movements, while open circles represent delayed submovements

maining one-third of the primary movements that were made as a single, uninterrupted movement, roughly 40% of these trials had a delayed submovement after the primary movement.

Kinematics of pure movements, unobscured by overlapping submovements

In the absence of submovements superimposed on the primary movement, the average angular position trajectory was sigmoidal with a near symmetric, bell-shaped angular velocity profile, like the trials of Fig. 1. The shape of the velocity profile was assessed with two values: K, representing the time symmetry or relative time to peak velocity of the movement, and C, representing the shape of the velocity profile as the ratio of peak velocity to mean velocity. Across subjects, the average K value for the single primary movements was 0.54, with an average subject standard deviation of 0.04. Thus the primary movements were close to symmetric, with a slightly longer acceleration time relative to deceleration time, and were consistently the same shape. The average C value for the six subjects was 1.58, with an average subject standard deviation of just 0.05.

Figure 4A,B shows the histograms of the symmetry index, K, and shape index, C, for all the single primary movements for subject SH. Although the symmetry index varied from trial to trial, the majority of trials were nearly perfectly symmetric for this subject. The shape index for each trial varied even less than the symmetry, with an average value of 1.58 for this subject.

In addition to the high regularity of an individual subject's kinematics, there was a uniformity of kinematics amongst the group of subjects. Despite the fact that the subjects performed differently and adopted different strategies in carrying out the knob-turning task, the symmetry and shape of their primary movements were remarkably similar. The set of mean K values for all six subjects was (0.50, 0.53, 0.55, 0.55, 0.55, 0.55), while the set of C values was (1.57, 1.57, 1.58, 1.59, 1.59, 1.61).

Panels C and D from Fig. 4 show delayed submovement K and C values from the same subject, while panels E and F pool all six subjects, with pure primary movement K and C values plotted versus speed. The cor-

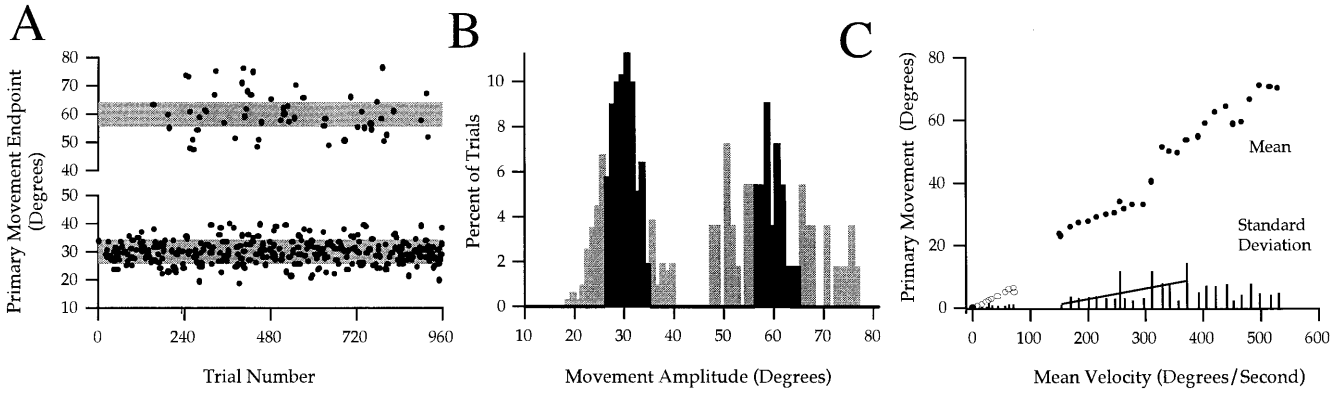

Fig. 5 **A** Scatter plot of subject JL's individual trial endpoints, defined as the position of the pointer when velocity decreased below 10% of the peak velocity, for movements without an overlapping submovement. **B** Histograms of primary movement endpoints, showing the larger variability in the 60° amplitude movements. The *black region* of the histograms represents accurate movements, those landing in the target zone. **C** Plot of primary movement (*filled circles*) and delayed submovement (*open circles*) amplitude mean and standard deviation as a function of the mean velocity. Each consecutive data point was calculated as the average and standard deviation of a group of trials over consecutive ranges of mean velocities

relation between the symmetry of the velocity profiles and the speed of each trial (Fig. 4E, r=0.023), and between the shape and speed (Fig. 4F, r=0.025), were insignificant. Similarly, there was no significant correlation between symmetry and movement time, r=0.05, and only a weak correlation between the shape and movement time, r=0.276. The subjects' pure primary movements thus had the same shape regardless of speed, duration, or amplitude of movement.

The accuracy of the pure primary movements are examined next. Figure 5A shows the pointer position at the end of each trial made as a single primary movement, for subject JL. The majority (211/310, 68%) of the 30° primary movements ended within the target zone, but only 40% (22/55) of the 60° movements ended in the target.

The primary movement endpoints were approximately normally distributed (Fig. 5B). Two types of errors were present: the variable error represents the spread of movement endpoints, or imprecision, while the constant, systematic, or mean error represents the average accuracy. In this subject, and four of the five others, there was a significant (P<0.001) difference between the 30° and 60° trials in the mean error of the primary movement endpoints. Subjects tended to overshoot the smaller targets slightly (average of 0.6° error), and undershoot the larger targets (average of –1.8° error). Likewise, there was a difference between the two amplitudes of movement in the variable error. For all subjects, the primary movement endpoint variability was higher in the 60° trials than the 30° ones. The very bottom two rows of Table 1 list some other differences between the smaller and larger amplitude movements. The subjects' larger movements had a larger peak velocity (588 versus 397°/s) and a slightly longer movement time (145 versus 127 ms). Figure 5B shows that subjects obeyed the general movement control principle of a speed–accuracy tradeoff: as they moved faster to cover twice as much distance in only 15% more time, movement variability increased.

A more direct way to examine the relationship between the speed and accuracy or variability of movements is to plot the standard deviation of the movement amplitude versus the mean velocity. Figure 5C shows this relationship graphically for the pure primary movements (filled circles) from subject JB. Although our experiment required only two categories of average velocity for the two amplitudes of movement (30° or 60°) with the same movement duration requirement, subjects naturally produced a wide range of mean velocities. After trials were sorted by mean velocity, the mean and standard deviation of the primary movement amplitude was computed over bins of trials with 16°/s widths. A line was fit to the data over the middle 88% of mean velocities, excluding trials in the extreme bins which contained too few trials to get a good sample. For this subject, the standard deviation was linearly proportional to mean velocity with a slope of 0.029. The r value for the fit was 0.92. For five of the six subjects, the range of slope values was 0.018–0.029, with an average of 0.021. One subject (SM) had a much lower slope value of 0.01, with all speeds of movement having a large amount of variability. The linear relationship between pure primary movement mean velocity and endpoint variability was significant (P<0.001) for all subjects.

Changes in kinematics with practice

As quantified in Table 1, the subjects initially made slow, inaccurate, and irregular movements, but during the practice session learned to make more rapid, accurate, and regular hand movements. Each column in Table 1 lists a different aspect of performance for each subject. The average performance metric at the beginning (average of first block of 240 trials) and end (last block of 240 trials) of the practice session is shown for each subject, with the six-subject average at the bottom. Significant changes (P<0.05; see Materials and methods) in a metric from the first run to the last are indicated

Table 1 Performance parameters for all subjects on the first and last run of 240 trials. Each *column* shows some aspect of performance, and each *row* lists the subject average on the first or fourth run. Significant changes in a metric are noted with an *underline*. Below the six individual subjects is the average of the six subjects for the first, second, third, and fourth run. The *final three rows* take the average metric for all trials, just the 30° ones, and just the 60° ones

Subject	Run	Trials	Percentage overlapping submovements	Percentage success	Mean Jerk^2 (10^9°/s^3)	Velocity error	Reaction time (ms)	Primary movement				
								Movement time (ms)	Peak velocity (°/s)	Mean endpoint error (°)	SD of endpoint error (°)	Percentage with delayed submovement
MB	1	239	74	72	3.0	28	209	207	402	0.9	3.2	42
	4	239	67	87	2.6	21	196	189	400	0.7	3.7	32
JB	1	240	75	4	6.2	43	317	201	387	–2.8	9.6	59
	4	240	74	27	5.3	42	235	196	440	–0.9	5.9	42
JG	1	238	74	27	7.1	284	284	193	457	–1.2	6.7	38
	4	240	63	44	6.0	265	265	173	480	–0.4	3.9	24
JL	1	240	67	42	3.0	30	247	199	385	0.5	6.0	21
	4	240	58	45	3.6	24	254	173	436	0.1	6.1	18
SM	1	237	77	7	13.2	43	366	188	528	–0.8	10.4	40
	4	240	79	22	16.0	36	277	182	605	0.5	8.3	43
SH	1	241	72	13	1.9	33	285	221	328	–2.2	12.3	23
	4	240	59	49	4.3	25	223	192	414	0.8	4.8	16
Average	1	239	73	28	5.7	77	285	201	415	–0.9	8.0	37
	2	240	67	35	7.0	72	260	187	467	0.2	6.2	35
	3	240	66	41	7.5	73	248	187	488	0.1	5.5	36
	4	240	67	46	6.3	69	241	184	463	0.1	5.4	29
All		239.7	68	37	6.6	73	258	190	458	–0.1	6.3	34
30°		161.3	59	44	5.7	69	264	172	396	0.6	4.9	32
60°		79.1	87	23	8.6	81	247	226	584	–1.8	7.8	39

with an underline for each subject. For instance, subject SH's percentage of trials with an overlapping submovement significantly decreased from 72 to 59% during the practice session. The first column in the table shows that the percentage of trials with a submovement superimposed on the primary movement decreased significantly in three of the six subjects, from an average (n=6) of 73% on the first run to 67% on the fourth run. In addition to decreasing the number of overlapping submovements, three of the six subjects made significantly fewer delayed submovements.

Task success (Table 1 column 5) significantly improved for all but one subject, from an average (n=6) of 28% correct trials on the first run to 46% on the last. Improvements in success rate appeared to slow near the end of the practice session, but, limited by subject fatigue, it is unknown whether subjects might have continued to improve with more practice.

Five of six subjects learned to react to the target LED illumination more quickly, significantly decreasing reaction time from an average (n=6) of 285 ms down to only 241 ms. In addition to initiating the movement sooner, four of six subjects significantly increased the primary movement peak velocity from an average (n=6) of 415 to 463°/s from the first to fourth runs during the training session. After subjects understood the rapid movement constraint, task success rates depended mainly on the consistency of hitting the target at the end of the primary movement. While learning to perform the task more quickly, subjects also made the movements more consistently. Four subjects had a significantly lower standard deviation of endpoint errors after practice, and the group average decreased from 8.0 to 5.4°. The mean of the distribution of endpoint errors improved significantly for two subjects, as the group average decreased from –0.9 to 0.1°.

The success rate varied greatly between subjects, ranging from 4% for the least successful block from a subject to 87% for the most successful subject. Table 1 shows that two subjects who were initially least successful at the task (JB and SM) had high standard deviations of the primary movement endpoint, indicating poor precision. In addition, both of the less successful performing subjects tended to make a large percentage (40–60%) of delayed submovements, often making unnecessary corrections that moved them out of the target. The final factor in low task success rate for the one subject was extremely high peak velocity (averaging 591°/s compared with the other five subjects' average of 432°/s) and a delayed reaction time (305 versus 249 ms for the others). Despite subject differences, and with one exceptional subject for each measure, all subjects improved task performance during practice by decreasing reaction time and moving with higher speed, accuracy, and precision.

Delayed submovement properties

When the primary movement did not land in the target zone, subjects often made delayed submovements, like the one in Fig. 1C. Table 1 shows that three of six subjects significantly decreased the percentage of trials in

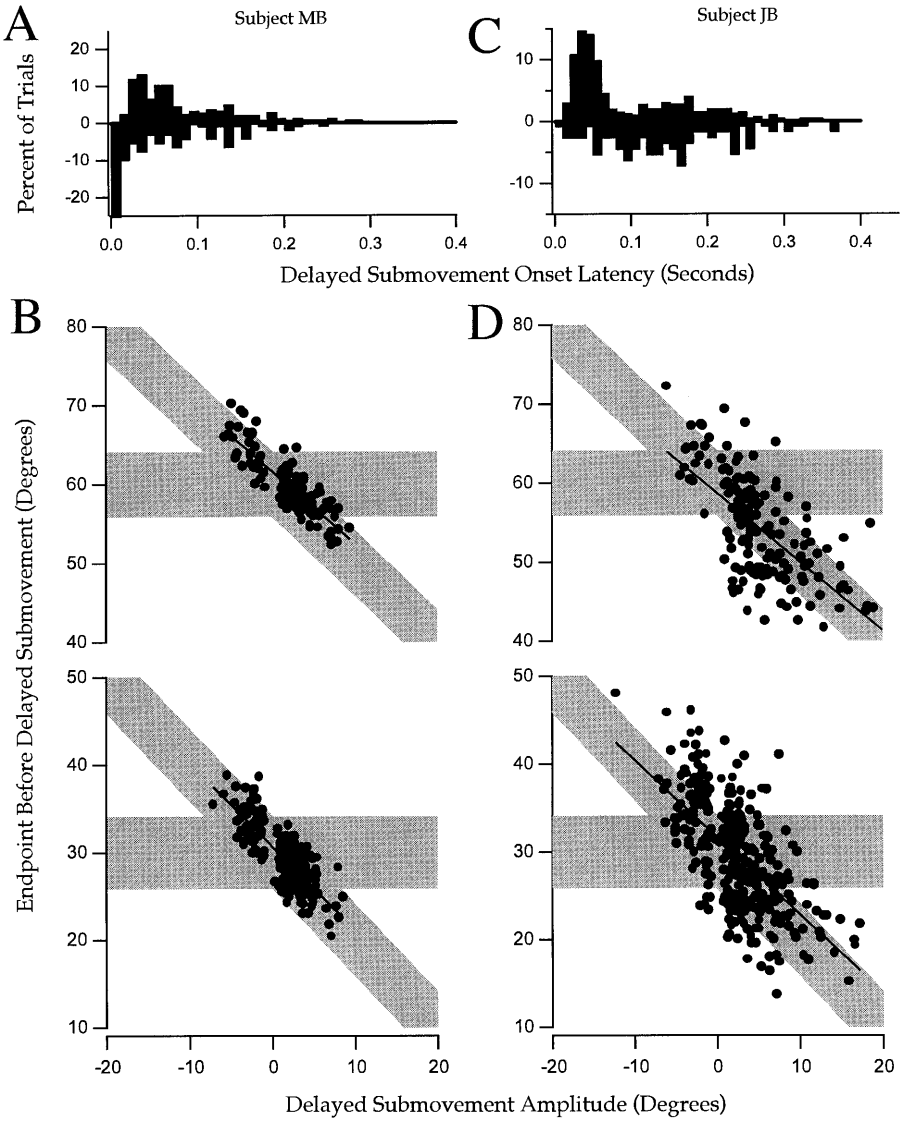

Fig. 6A–D Latency and effectiveness of delayed submovements for two subjects, MB (*left column*) and JB (*right column*). **A,C** Histograms of onset latency of delayed submovement after initial movement settled to zero. Submovements in the same direction as the primary movement are shown above the *x*-axis and submovements in the other directions below the *x*-axis. **B,D** Scatter plots of endpoint before delayed submovement versus amplitude of delayed submovement. Perfectly corrective submovements lie along a line in the middle of the *diagonal shaded region*. Trials in the *diagonal shaded region* ended in the target zone

which they made delayed corrections, from a six-subject average of 37% down to 29%. Similar to the analysis of the primary movements, the higher-order kinematics of the delayed submovements were examined for their regularity in terms of jerk and snap zero crossings. Across all subjects, 32.5% of the delayed submovements were irregular, with one or more overlapping submovements.

The symmetry (K) and shape (C) coefficients of the velocity profiles of the regular, uncontaminated delayed submovements were computed as they were for the regular primary movements. The average K value for the delayed submovements from all subjects was 0.51, with an average standard deviation of 0.07. The shape coefficient averaged 1.58, with an average standard deviation of 0.16. Figure 4C,D shows that the distribution of shape and symmetry values for subject SH was more disperse compared with the primary movements of Fig. 4A,B, but have roughly the same mean. The increased variability may be due to undetected overlapping submovements on top of the small amplitude delayed submovement. For whatever reason, the shape of the delayed submovements was less stereotypical, but in the average still retained the symmetric, bell-shaped velocity profile of the primary movements.

The average amplitude of the delayed submovements (3.51°) was much smaller than that of the primary movements, with a lower peak velocity (48.8°/s) as well as a shorter movement time (86.4 ms). The delayed submovements ranged in onset latency from immediately after the original movement settled to zero, up to 400 ms after this time. Figure 6A,C shows histograms of onset latency for two subjects. Across all subjects, the average delay was 76 ms, with a wide range like the two subjects shown.

The speed–accuracy relationship of pure delayed submovements is shown in Fig. 5C, open circles. For the subject illustrated, the average mean velocity was very small, at 25°/s, with a small standard deviation as well, at 0.84. However, the slope of the line fit through the standard deviation of the delayed submovement ampli-

tude versus the mean velocity was very close to that of the primary movement, with a value of 0.019° of standard deviation per degree per second of mean velocity. As the delayed submovements were made faster, there was more variability in their amplitudes.

The delayed submovements were corrective in nature, compensating for errors in the end position of the pointer on a trial by trial basis. The standard deviation of the endpoint position improved after the correction (from 6.1 to 4.8°), as did the mean endpoint error (from a 1.2° undershoot to a 0.7° overshoot). The improvement in the set of 60° trials was more dramatic. The average endpoint error improved from a 3.7° undershoot to a 0.4° undershoot.

Figure 6B,D examines the effectiveness of the delayed submovements more closely by plotting the knob pointer end position before the delayed submovement versus the amplitude of the submovement for two subjects. Subject MB is shown on the left and subject JB on the right, while the 60° trials are separated from the 30° trials below them. If the knob pointer was supposed to reach the target 30° away but instead only made it 20°, a corrective submovement of 10° was required to land the pointer perfectly on the target center. The amplitudes of the corrective submovements were inversely related to the endpoint errors for all subjects. A line fit through hypothetical perfect submovements would have a slope of –1.0 and an *r* of –1.0. The linear least-squares fit for the 30° trials of subject MB has a slope of –0.95 and an *r* of –0.80, while the 60° trial fit has a slope of –0.91 and an *r* of –0.74. Subject JB's delayed corrections were less accurate. The line through the 60° trials has a slope of –0.87 and an *r* of –0.72. The slope of the 30° trial fit is –0.88, with a poorer fit (r=–0.63). Across subjects, the average slope was –1.03, and the average *r* was –0.64. The amplitude of the corrections were well tuned for final endpoint accuracy.

The diagonal shaded region represents the range of amplitudes of the delayed submovement that would reach the target, an accurate correction. A large majority of the delayed submovements lay within this region and thus accurately corrected for errors in the amplitude of the original movements. For instance, subject MB made 90% of the delayed submovements within the diagonal shaded region. Subject JB performed significantly worse than subject MB, with both a decrease in endpoint precision before the delayed submovement (increased vertical dispersion), and in the accuracy of the delayed corrective submovement, with only 55% of trials inside the diagonal shaded region. Of all the delayed submovements from all subjects, 62% ended inside the target.

Another measure of the accuracy of the submovements was the direction of the correction, whether or not the submovements moved the pointer towards the target (upper left or lower right quadrants) or away from the target (upper right and lower left quadrants). Across subjects, over 78% of the submovements were made in the appropriate direction, moving the pointer towards the target.

Two final measures of the correctness of the delayed submovements were trials in which subjects did not move and should have, i.e., they were out of the target but stayed there, and when they moved and should not have, i.e., they were in the target but moved out of it. On average, subjects did not make a delayed submovement on 26% of the trials when they should have, and on 9% of the trials made submovements moving them out of the target.

On the whole, the subjects' delayed submovements were very good considering they were made without visual feedback. The delayed submovements were made with the same symmetric, bell-shaped velocity profiles as the single primary movements, although slightly more variable, and acted to improve the final endpoint accuracy of the movements.

Possible origins of variable movement symmetries – modeling results

Figure 4 showed that on average, the single primary movements were symmetric, with a small amount of variability in the symmetry index. However, there was a range of symmetry values, with example velocity profiles shown in Fig. 7A: the typical symmetric trial (thick, K=0.52), an extreme low symmetry trial (thin, K=0.37), and an extremely high symmetry trial (dashed, K=0.63). The exceptionally asymmetric trials may be explained by one of several potential mechanisms that changes the strength of the antagonist braking torque pulse relative to the agonist accelerating torque pulse. Two possibilities include changing central commands to the agonist and/or antagonist muscle sets, and changing the effective limb impedance through co-contraction. These possibilities are examined with a model of the motor plant, detailed in the Materials and methods section.

Basically, the model has a mass, spring, and nonlinear damping. It is based on equilibrium point control theory (Bizzi et al. 1984; Feldman 1986), pulse-step control of limb movements, and observations of fractional power viscous damping (Gielen et al. 1984; Wu et al. 1990) due to the stretch reflex. Although the model was originally formulated to describe motion of the human wrist, the principles of control and the mechanics of the model can be applied conceptually to the complicated finger and wrist turning motion studied in this task. The model output of position of the mass at the end of the spring over time can be treated as the length of a muscle. Making the simplification that the muscle generates moments about a revolute joint with a constant moment arm and that the tendon wraps around a circular joint, the muscle length is linearly related to the joint angle. While expressed in centimeters, the output of the model may be conceptualized as the angular position of the knob pointer studied in this task.

In Fig. 7B a filtered, centrally generated pulse-step command, corresponding to the slack length of the spring or the threshold of the stretch reflex, is shown along with the resulting movement of the mass from 0 to

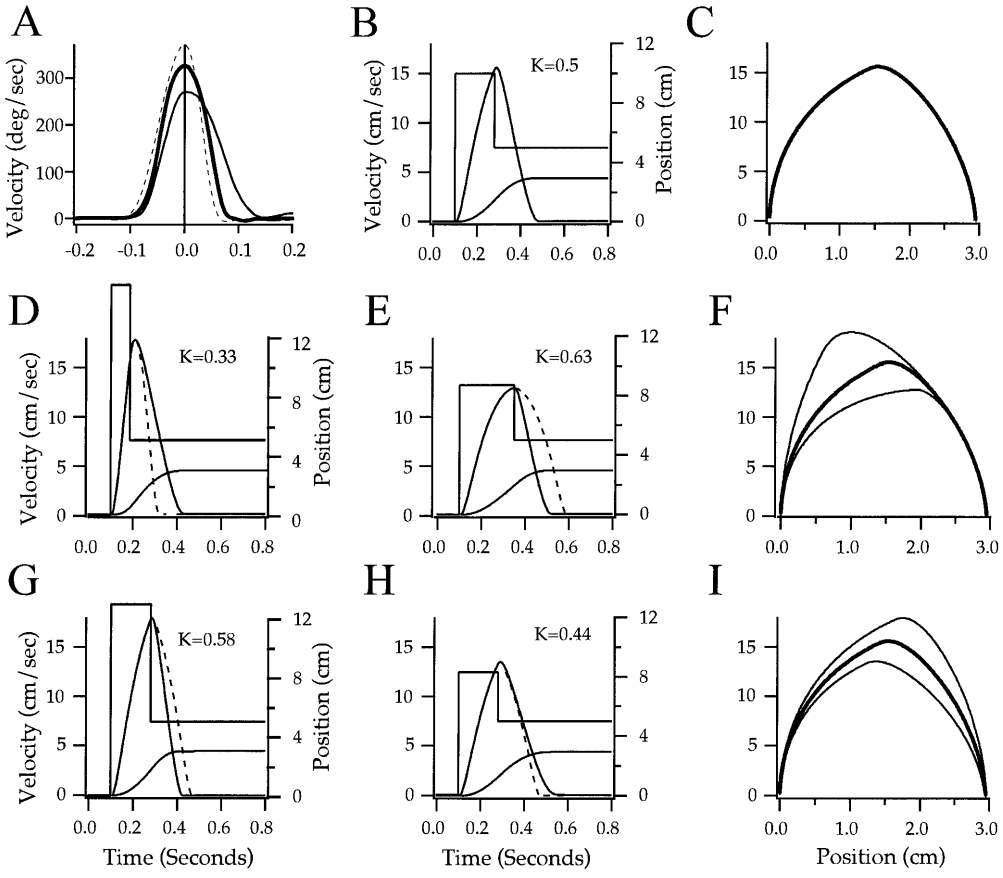

Fig. 7 Simulations showing how varying pulse parameters (**D–F**) or modifying the non-linear damping parameter b (**G–I**) may change the symmetry of the movements, to describe some of the natural variability (**A**). **A** Three single primary movement velocity profiles with different symmetry values: K=0.5 (*thick*), K=0.37 (*thin*), and K=0.63 (*dashed*). **B** Simulation results for a pulse-step command into a non-linear viscous damping, mass-spring model of movement. **C** Phase plane trajectory of movement in **B**, plotting velocity versus position. **D** A large amplitude, short duration pulse command, resulting in a movement of the correct amplitude, but with a symmetry value smaller than normal (*dashed line* is a symmetric movement). **E** A small amplitude, wide duration pulse results in a correct final position endpoint, but an asymmetric velocity profile with K larger than normal. **F** Phase-plane trajectories of **D** (*top*), **E** (*bottom*), and the normal movement of **B** (*middle*). Note that as K increased, the peak velocity also increased. **G** Non-linear damping parameter b increased to 4 from 3. The movement amplitude was correct, but the symmetry value of the movement increased, with the movement decelerating quicker than normal (*dashed line*). **H** Decreased b from 3.0 to 2.5. The resulting velocity profile took longer during the deceleration phase, K=0.44. Note that as the peak velocity of the movements increased, so did the K values. **I** The phase-plane trajectories of **G** (*top*), **H** (*bottom*), and the normal **B** (*middle*)

2.96 cm. The sigmoidal position trace fell short of the final commanded equilibrium position of 5 cm because the fractional power viscosity caused the mass to stick at a low velocity near the end of the movement. The shape of the velocity profile for this movement was near bell-shaped and perfectly symmetric, with a relative time to peak velocity (K) of 0.50. Figure 7C shows the movement trajectory in the phase plane.

The simulations of Fig. 7D–F explore how changing the pulse-step parameters changes the symmetry of a single primary movement. In Fig. 7D a large amplitude, narrow pulse command generated a movement that reached the same final position as the previous movement at 2.96 cm using the same final step command of 5 cm. The shape of the velocity profile, however, was much different. The peak velocity was higher by around 2 cm/s and the relative time to peak velocity, K=0.33. In this movement, acceleration was very rapid and deceleration took twice as long. The dashed line on the velocity profile was generated by flipping the profile about its peak in a mirror-like fashion and shows what the velocity would look like if it were symmetric. Symmetry can be shifted in the other direction by using a smaller amplitude pulse for a longer duration. In Fig. 7E, again the correct amplitude of movement was achieved with a different shape velocity profile. Here acceleration time was prolonged and deceleration was relatively short, resulting in a K value of 0.63, with the peak velocity occurring relatively late in the movement.

Figure 7F shows the phase-plane trajectories for the previous two movements with asymmetric velocity profiles along with the phase-plane trajectory of a perfectly symmetric movement (heavy trace). One problem with this simple simulation is that one cannot control the shape of the movement velocity profile while keeping the peak velocity and movement time the same. As the peak velocity increased, less time was spent in acceleration and K decreased.

In the phase-plane (Fig. 7F), each of the three simulated movements with different symmetries descended along the same trajectory. One way to increase how quickly a movement is stopped is to change the way it descends on the phase plane, by increasing the nonlinear damping parameter, b. When b was increased by 33% in the simulation of Fig. 7G, a larger amplitude pulse was required to achieve a movement of the same amplitude. The peak velocity increased and occurred relatively later in the movement, yielding K=0.58. The movement ended abruptly, like the experimental trial (dashed trace) of Fig. 7A. Figure 7H shows a movement with the damping parameter decreased by one-sixth. With less damping, a smaller command pulse was needed to generate a movement of 2.96 cm. The peak velocity in this case was decreased, and the symmetry was shifted to K<0.5, with a longer deceleration time with respect to acceleration time. The three movements with different viscous damping coefficients and different gains of stretch reflex are shown in the phase-plane in Fig. 7I. In contrast to Fig. 7F, the three trajectories of Fig. 7B,G,H descend along different curves in the phase plane. The symmetry versus speed relationship is reversed for these simulations where the damping coefficient was changed, compared to the simulations where pulse parameters were changed. As movements were made faster, the K value increased.

Discussion

Subjects rapidly twisted the knob pointer towards the LED targets with a large primary movement, and often one or more additional submovements during or after the primary movement. We devised a direct, objective algorithm to detect when a submovement overlapped the primary movement or a delayed submovement, and then performed an analysis of the properties of those pure movements without overlapping submovements.

The regularity of movements and overlapping submovements

Our interpretation that irregularities in the kinematics of movements are caused by discrete overlapping submovements follows the work of many other movement studies (Flash and Henis 1990; Milner 1992) that have put forth a similar explanation. Prior studies generally involved iteratively fitting and subtracting a scaled velocity template from successive velocity peaks until there was no velocity remaining to fit (Berthier 1996; Flash and Henis 1990; Lee et al. 1997; Milner 1992). These studies detected the presence of overlapping submovements either indirectly, with least-squares curve fitting, or subjectively, with guesses for initial parameters (Lee et al. 1997) or for submovement timing and amplitude parameters (Milner 1992). Only one study (Milner 1992) used a set of heuristics based on velocity inflections, zero crossings, and changes of direction to determine when an overlapping submovement was present. Our approach to detecting overlapping submovements was completely objective, assuming only that single movements without overlapping submovements should have smooth and regular accelerations, with only one jerk and one snap zero crossing during the second half of a movement.

Despite the success of past studies, there remains some controversy over the idea of movement segmentation, with some holding that what appear to be discrete segments in a movement may instead be the result of a single continuous motor process dynamically interacting with the environment (Kawato 1992; Shadmehr and Mussa-Ivaldi 1994) or a property of the neuromusculoskeletal system itself (Plamondon and Alimi 1997).

If the musculoskeletal system oscillates like a simple, underdamped, third-order system, movements like we simulated in Fig. 2F should be seen. However, the majority of movements had no oscillation whatsoever, but smoothly settled into the final position. In some cases there was a single correction in the opposite direction when the initial movement overshot the target, as in Fig. 2C. Instead of an underdamped oscillation, we interpret this irregularity as an overlapping submovement, acting to brake the primary movement more strongly.

The variability of the onset time of delayed submovements and the presence of “dead time” between movements indicate that some variable brain process is acting to adjust the final position of the knob pointer, by issuing a discrete corrective command to the muscles. Evidence for such central commands preceding corrective submovements has been found in studies of single neurons in the red nucleus of monkeys performing various forelimb motor tasks (Gibson et al. 1985, Fig. 2D; Miller and Houk 1995).

We propose that two brain processes are responsible for planning and controlling movements: one to initiate the primary movement and corrective submovements, and one to regulate and tune the parameters. The initiator process might be realized by a circuit between the basal ganglia, thalamus, and motor cortical areas, and the regulator process by a loop between the motor cortical areas, red nucleus, pons, thalamus, and the cerebellum (Houk et al. 1993). Corrective submovements may be generated by evaluating efference copy and afferent feedback. These circuits could form functional modules which interact together to control movements (Houk and Wise 1995).

Shape of movement kinematics

The rapid hand movements studied in this task were quite complicated, requiring considerable coordination between the four fingers, thumb, and wrist. It was remarkable that this complex, multi-degree of freedom hand movement was often made with such a simple, smooth trajectory. On the trials determined to be without any overlapping submovements, the shape of the angular

position over time was sigmoidal, and the velocity was, on average, the symmetric bell-shape that has been reported in numerous human movement studies (Abend et al. 1982; Atkeson and Hollerbach 1985; Flash and Hogan 1985; Gordon et al. 1994; Morasso 1981; Uno et al. 1989).

The pure primary movements and the pure delayed submovements had exactly the same mean shape, each with an average C value of 1.58 across subjects. Both were very nearly symmetric, with K values of 0.54 for the primary movements and 0.51 for the delayed submovements. The shape varied little from trial to trial, and was very close to the minimum jerk velocity profile (K=0.5, C=1.57, using 10% of peak velocity start and stop criteria).

Unlike other studies (Moore and Marteniuk 1986; Nagasaki 1989; Wiegner and Wierzbicka 1992), we found that neither the shape nor the symmetry of the movements were dependent on speed or movement duration (Fig. 4C,D). Speed-related velocity asymmetry in other studies may have resulted from trials that contained overlapping submovements. These submovements could act either to hasten or prolong the deceleration phase of the movement, changing the movement symmetry. Since we excluded those trials with overlapping submovements, we did not find speed-dependent changes in the shape of the velocity profile.

Explanations for movement asymmetries

The inclusion of overlapping submovements is one reason that movements may become asymmetric. In order to explore other possibilities for generating asymmetric velocity profiles, we simulated a simple mass-spring system with non-linear damping and pulse-step control (see Materials and methods). Two mechanisms for altering the kinematics of a movement are to change the central pulse command parameters and to change the mechanical impedance of a joint. The central nervous system may alter mechanical impedance by coactivation of agonist–antagonist muscle pairs to alter the stretch reflex (Feldman 1986; Houk and Rymer 1981) and muscle mechanical properties (Hogan 1990), or possibly by changing the gain of the stretch reflex (Edamura et al. 1991). We simulated a change in mechanical impedance in our model by changing the non-linear damping parameter, b. Increasing b caused the movement to decelerate more rapidly, while decreasing b caused a slower deceleration, with corresponding changes in symmetry.

Alternatively, increasing the size and reducing the duration of the pulse-step command caused the relative velocity peak to be shifted to the left. Conversely, a relatively small, long duration pulse caused the peak to be shifted to the right. These simulation results qualitatively match those reported in a study of triphasic EMG burst activity in rapid elbow flexions by Brown and Cooke (1990). In that study, subjects were guided to make a given movement with different velocity profile symmetries, ranging from around 0.3 to 0.7. As K increased, the agonist EMG pulse went from a large amplitude and short duration to a small amplitude and long duration, just as in our simulation of the central command pulse.

In our model, the pulse portion of the central command is best related to the initial agonist muscle activity. Although the antagonist muscle is not explicitly represented, it is incorporated in the stretch reflex and the fractional power damping, which produce the antagonist muscle braking pulse. Past experimental (Ghez and Martin 1982) and simulation (Ramos and Stark 1987) studies are consistent with this notion that the antagonist braking activity may be caused by the stretch reflex, instead of or in addition to a central command. A further elaboration of the fractional power damping model into a six-muscle, two-joint arm (Houk et al. 2000) is able to reproduce a triphasic EMG pattern with a pulse-step central command and spinal reflexes.

Although the model used here is simple, it captures some important properties of the musculoskeletal system. It recently has been used to describe how changing the duration of the pulse leads to the linear relationship between the peak speed and amplitude of movement, and the log relation of movement duration versus movement amplitude (Karniel and Inbar 1999). The control parameters of the model, the pulse-step activation, relate well to central neural commands actually measured in the motor cortex (Lamarre et al. 1983) and red nucleus (Gibson et al. 1985), and to muscle activity (Gottlieb et al. 1989). The task of the motor controller may be described as learning and choosing the appropriate pulse parameters to activate the muscles (Barto et al. 1999; Karniel and Inbar 1997).

Movement variability

Whatever the neural basis of moving with a near symmetric, bell-shaped velocity profile, the nervous system cannot repeatedly produce this movement precisely. Nor can the nervous system consistently produce the same movement amplitudes or endpoints. This variability in movement positioning increases as movements are made faster. This so-called speed–accuracy tradeoff has been studied extensively (Fitts 1954; Meyer et al. 1988; Plamondon and Alimi 1997; Woodworth 1899). Empirical laws have been formed describing the relationship as logarithmic (Fitts 1954) or linear (Schmidt et al. 1979). Our data obeyed the linear speed–accuracy tradeoff: the standard deviation of movement amplitude was linearly proportional to the mean velocity (Fig. 5C). The linear coefficient averaged 0.021 s across subjects, similar to the values of around 0.025 of Meyer et al. (1988, approximated from Fig. 8) and 0.024 reported by Burdet and Milner (1998).

Several investigators have incorporated the speed–accuracy notion into models of submovement generation (Burdet and Milner 1998; Meyer et al. 1988) or attempted to explain it as a driving force in planning and con-

trolling movements (Harris and Wolpert 1998). Our data are consistent with the submovement models, in that subjects make corrective submovements to deal with noisy and variable amplitude primary movements. As has been observed previously (Crossman and Goodeve 1983; Milner 1992), the subjects used the strategy of more corrective submovements when the relative difficulty was greater for the 60° trials. The delayed submovements corrected for primary movement errors, increasing the final endpoint accuracy while reducing the endpoint variability.

It is interesting that through practice the subjects learned to make less variable primary movements. Two successful theoretical models of motor learning (Barto et al. 1999; Berthier et al. 1993; Kawato and Gomi 1993) depict the goal of the adaptive motor controller to reduce the need for feedback-based corrections, producing a single movement accurately in a feedforward manner. The task of the central nervous system in motor control would then be to activate the muscles synergistically, turning certain muscles on and off at the proper time to generate a single, smooth, and accurate movement with maximal speed and minimal effort, a movement which does not require a correction. As infants develop (Berthier 1997), stroke patients recover (Krebs et al. 1998), and subjects practiced a movement task, people learn to make more accurate movements requiring fewer corrective submovements.

However, when faced with the limits of variability in fast movements, it may be a better strategy to allow a submovement to complement a variable amplitude primary movement (Meyer et al. 1988). The nervous system seems to be driven by two competing forces: one to produce a single, smooth, accurate, time optimal movement without discrete corrective submovements, and another to compensate for the variability inherent in rapid movements, producing the best strategy of corrective submovements that maximizes final accuracy and minimizes total movement time.

References

Abend W, Bizzi E, Morasso P (1982) Human arm trajectory formation. Brain 105:331–348

Atkeson CG, Hollerbach JM (1985) Kinematic features of unrestrained vertical arm movements. J Neurosci 5:2318–2330

Barto AG, Fagg AH, Sitkoff N, Houk JC (1999) A cerebellar model of timing and prediction in the control of reaching. Neural Comput 11:565–594

Berthier NE (1996) Learning to reach: a mathematical model. Dev Psychol 32:811–823

Berthier NE (1997) Analysis of reaching for stationary and moving objects in the human infant. In: Donahue J, Dorsal VP (eds) Neural network models of complex behavior – biobehavioral foundations. North Holland, Amsterdam, pp 283–301

Berthier NE, Singh SP, Barto AG, Houk JC (1993) Distributed representation of limb motor programs in arrays of adjustable pattern generators. J Cog Neurosci 5:56–78

Bizzi E, Accornero N, Chapple W, Hogan N (1984) Posture control and trajectory formation during arm movement. J Neurosci 4:2738–2744

Brown SH, Cooke JD (1990) Movement-related phasic muscle activation. I. Relations with temporal profile of movement. J Neurophysiol 63:455–464

Buckingham JT, Houk JC, Barto AG (1994) Controlling a nonlinear spring-mass system with a cerebellar model. In: Proc Eighth Yale Workshop on Adaptive and Learning Systems. Yale University Press, New Haven

Buckingham JT, Barto AG, Houk JC (1995) Adaptive predictive control with a cerebellar model. Proc World Congr Neural Networks. Erlbaum, Hillsdale

Burdet E, Milner TE (1998) Quantitation of human motions and learning of accurate movements. Biol Cybern 78:307–318

Crossman ERFW, Goodeve PJ (1983) Feedback control of hand-movement and Fitts' Law. Q J Exp Psychol A 35:251–278

Edamura M, Yang JF, Stein RB (1991) Factors that determine the magnitude and time course of human H-reflexes in locomotion. J Neurosci 11:420–427

Feldman AG (1986) Once more on the equilibrium-point hypothesis (lamda model) for motor control. J Mot Behav 18:17–54

Fitts PM (1954) The information capacity of the human motor system in controlling the amplitude of movement. J Exp Psychol 47:381–391

Flash T, Henis E (1990) Arm trajectory modifications during reaching towards visual targets. J Cog Neurosci 3:220–230

Flash T, Hogan N (1985) The coordination of arm movements: an experimentally confirmed mathematical model. J Neurosci 5: 1688–1703

Ghez C, Martin JH (1982) The control of rapid limb movement in the cat. III. Agonist–antagonist coupling. Exp Brain Res 45:115–125

Gibson AR, Houk JC, Kohlerman NJ (1985) Relation between red nucleus discharge and movement parameters in trained macaque monkeys. J Physiol 358:551–570

Gielen CC, Houk JC, Marcus SL, Miller LE (1984) Viscoelastic properties of the wrist motor servo in man. Ann Biomed Eng 12:599–620

Gordon J, Ghilardi MF, Ghez C (1994) Accuracy of planar reaching movements. I. Independence of direction and extent variability. Exp Brain Res 99:97–111

Gottlieb GL, Corcos DM, Agarwal GC (1989) Strategies for the control of voluntary movements with one mechanical degree of freedom. Behav Brain Sci 12:189–250

Harris CM, Wolpert DM (1998) Signal-dependent noise determines motor planning. Nature 394:780–784

Hogan N (1990) Mechanical impedance of single- and multi-articular systems. In: Winters JM, Woo SL-Y (eds) Multiple muscle systems: biomechanics and movement organization. Springer, Heidelberg Berlin New York, pp 150–164

Houk JC, Rymer WZ (1981) Neural control of muscle length and tension. In: Brooks VB (ed) Handbook of physiology, Vol II. The central nervous system II. American Physiological Society, Bethesda, pp 257–323

Houk JC, Wise SP (1995) Distributed modular architectures linking basal ganglia, cerebellum, and cerebral cortex: their role in planning and controlling action. Cereb Cortex 5:95–110

Houk JC, Keifer J, Barto AG (1993) Distributed motor commands in the limb premotor network. Trends Neurosci 16:27–33

Houk JC, Barto AG, Fagg AH (2000) Fractional power damping model of joint motion. In: Latash ML (ed) Progress in motor control: structure-function relations in voluntary movements, vol 2. Human Kinetics, Champaign (in press)

Karniel A, Inbar GF (1997) A model for learning human reaching movements. Biol Cybern 77:173–183

Karniel A, Inbar GF (1999) The use of a nonlinear muscle model in explaining the relationship between duration, amplitude, and peak velocity of human rapid movements. J Mot Behav 31:203–206

Kawato M (1992) Optimization and learning in neural networks for formation and control of coordinated movement. In: Meyer D, Kornblum S (eds) Attention and performance, vol XIV. MIT Press, Cambridge, Mass., pp 821–849

Kawato M, Gomi H (1993) Feedback-error-learning model of cerebellar motor control. In: Mano N, Hamada I, DeLong MR Role of the cerebellum and basal ganglia in voluntary movement. Elsevier Science Publishers, Amsterdam, pp 51–61

Keele SW (1968) Movement control in skilled motor performance. Psychol Bull 70:387–403

Krebs HI, Hogan N, Aisen ML, Volpe BT (1998) Robot-aided neurorehabilitation. IEEE Trans Rehabil Eng 6:75–87

Lamarre Y, Busby L, Spidalieri G (1983) Fast ballistic arm movements triggered by visual, auditory, and somesthetic stimuli in the monkey. I. Activity of precentral cortical neurons. J Neurophysiol 50:1343–1358

Lee D, Port NL, Georgopoulos AP (1997) Manual interception of moving targets. II. On-line control of overlapping submovements. Exp Brain Res 116:421–433

Meyer DE, Abrams RA, Kornblum S, Wright CE, Smith JE (1988) Optimality in human motor performance: ideal control of rapid aimed movements. Psychol Rev 95:340–370

Miller LE, Houk JC (1995) Motor co-ordinates in primate red nucleus: preferential relation to muscle activation versus kinematic variables. J Physiol 488:533–548

Milner TE (1992) A model for the generation of movements requiring endpoint precision. Neuroscience 49:487–496

Moore SP, Marteniuk RG (1986) Kinematic and electromyographic changes that occur as a function of learning a time-constrained aiming task. J Mot Behav 18:397–426

Morasso P (1981) Spatial control of arm movements. Exp Brain Res 42:223–227

Morasso P, Mussa Ivaldi FA (1982) Trajectory formation and handwriting: a computational model. Biol Cybern 45:131–142

Nagasaki H (1989) Asymmetric velocity and acceleration profiles of human arm movements. Exp Brain Res 74:319–326

Novak KE, Miller LE, Baker JF, Houk JC (1996a) Optimization criteria driving adaptation in manipulative hand movements. Soc Neurosci Abstr 22:898

Novak KE, Miller LE, Houk JC (1996b) Biological mechanism for optimal motor control. In: Ninth Yale Workshop on Adaptive and Learning Systems. Yale University Press, New Haven, pp 201–206

Plamondon R, Alimi AM (1997) Speed/accuracy trade-offs in target-directed movements. Behav Brain Sci 20:1–31

Pratt J, Chasteen AL, Abrams RA (1994) Rapid aimed limb movements: age differences and practice effects in component submovements. Psychol Aging 9:325–334

Ramos CF, Stark LW (1987) Simulation studies of descending and reflex control of fast movements. J Mot Behav 19:38–61

Schmidt RA, Zelaznik H, Hawkins B, Frank JS, Quinn JT Jr (1979) Motor-output variability: a theory for the accuracy of rapid motor acts. Psychol Rev 47:415–451

Shadmehr R, Mussa-Ivaldi FA (1994) Adaptive representation of dynamics during learning of a motor task. J Neurosci 14: 3208–3224

Soechting JF (1984) Effect of target size on spatial and temporal characteristics of a pointing movement in man. Exp Brain Res 54:121–132

Uno Y, Kawato M, Suzuki R (1989) Formation and control of optimal trajectory in human multijoint arm movement. Minimum torque-change model. Biol Cybern 61:89–101

Wiegner AW, Wierzbicka MM (1992) Kinematic models and human elbow flexion movements: quantitative analysis. Exp Brain Res 88:665–673

Woodworth RS (1899) The accuracy of voluntary movement. Psychol Rev 3:1–114

Wu C-H, Houk JC, Young KY, Miller LE (1990) Nonlinear damping of limb motion. In: Winters JM, Woo SL-Y (eds) Multiple muscle systems: biomechanics and movement organization. Springer, Heidelberg Berlin New York, pp 214–235